Materials Research Proceedings **26** (2023) 659-664 https://doi.org/10.21741/9781644902431-106

Dynamic analysis of lightweight gears through multibody models with movable teeth

Marco Cirelli [1,a*], Alessio Cellupica [2,b], Mattia Cera [2,c], Oliviero Giannini [1,d], Pier Paolo Valentini [2,e], Ettore Pennestrì [2,f]

[1] Department of mechanical engineering, University Niccolò Cusano, Rome, Italy

[2] Department of enterprise engineering, University of Rome Tor Vergata, Rome, Italy

[a]marco.cirelli@unicusano.it, [b]alessio.cellupica@alumni.uniroma2.eu, [c]mattia.cera@uniroma2.it, [d]oliviero.giannini@unicusano.it, [e]valentini@ing.uniroma2.it, [f]pennestri@mec.uniroma2.it

Keywords: Lightweight Gears, Pseudo Rigid Teeth, Contact

Abstract. This paper aims the study of lightweight gears through a novel approach based on a multibody model contact-based with pseudo-rigid teeth. This method considers the teeth as pseudo-rigid bodies attached to the main body through revolute joints and torsion springs with precomputed stiffness. Thanks to this approach, the lightening is considered by varying the value of the stiffness parameter. To validate the method, the first step compares the Transmission Error computed with this novel approach with the Finite Element method in quasi-static operating conditions. The second step highlights the behaviour of the Transmission Error, increasing the rotation speed.

Introduction

Lightweight gears (LGs) represent one of the most common design solutions to increase the efficiency of the transmission system. This approach is based on the reduction of inertia properties that generates a decrease in the potential energy dissipated in the transient phase. Lightening is produced by reducing the gear rim thickness or by introducing holes on the gear rim. Recently many researchers have found solutions to consider the effects on the transmission error (TE) introduced by lightening. In reference [1], the dynamic behaviour of LG is investigated through a one degree-of-freedom (DOF) considering a time depending on mesh stiffness (MS) computed through the Finite Element (FE) method. This approach is well documented in the literature and remains widely adopted at the design level. In reference [2], the TE and the strain analysis of LGs are obtained by using a hybrid FE-analytical gear contact model. The weakness of the analytical approach is that the MS needs be previously computed through FE models. For this reason, a multibody model contact-based with pseudo-rigid tooth (MUBOCO-PR) has been introduced [3, 4]. This method considers the teeth as pseudo-rigid bodies attached to the main body through revolute joints and torsion springs having a precomputed stiffness. In this way, the flexibility of the tooth and the gear body can be condensed into the torsion spring. This approach has been already adopted for gears having tip relief modifications [5]. The main purpose of this investigation is to show how this method can be extended to the study of the LGs. To simplify the interpretation of the numerical results, and consistently with the findings reported in [6], it is introduced the definition of the transmission error (TE) as "*the deviation in position of the driven gear and the position it would occupy if the gear drive were perfectly conjugate*". Using the subscript s 1 and 2 to denote the driving and the driven gear, respectively, the TE along the line of action in an ordinary gear train is expressed as

$$TE(t) = r_{b1}\theta_1(t) + r_{b2}\theta_2(t) \tag{1.1}$$

for the *i*-th gear (*i=1,2*), $\theta_i(t)$ is the angular position, measured from the nominal position, and r_{bi} the base radii, respectively.

If the TE is measured in static conditions, it can be defined as Static transmission error (STE). Conversely, if it is evaluated under operating conditions, it is termed dynamic transmission error (DTE). While the STE depends on compliance contributions of the system and geometrical properties of the profile, the dynamic response involves phenomena such as impacts, nonlinear effects, and vibrations. The paper is organized as follows: in the first part, a general methodology to generate a MUBOCO-PR model is presented. Then, STE numerical results have been compared with FE model in quasi-static conditions.

Method

MUBOCOF-PR, considers each tooth as an individual body elastically connected to the gear hub through a specific elastic joint, considering the elastic contributions that represent the source of excitation of the system. In particular, the rim body and the teeth compliances are condensed into specific spring joints, while the contact compliance is assigned to the contact stiffness. In this way, a suitable separation of all the described contributions can be achieved.

The parameters to be specified are load conditions, stiffness, and damping for the spring at each tooth joint and the parameters for the multibody contact formulation. The generalized spring force is computed by means of the following equation:

$$T_{junction} = -k_\varphi(\varphi-\varphi_0)^{n_{k\varphi}} - c_\varphi\dot{\varphi}^{n_{c\varphi}} + T_0 \tag{1.2}$$

where k_φ and c_φ are the spring stiffness and damping coefficients, respectively; $n_{k\varphi}, n_{c\varphi}$ the exponents of the relative rotation and angular velocity, respectively; T_0 the free length spring torque; φ the angle of the current rotation; φ_0 the free angle. Assuming T_0=0 and φ_0=0, only four parameters, namely $k_\varphi, c_\varphi, n_{k\varphi}, n_{c\varphi}$, need to be identified.

The contact formulation adopted in this work is based on a double detection phase: pre-search to identify contact zones and a detailed search to find the penetration depth of the contact regions [7]. A 2D contact model without friction has been used to estimate the penetration depth with a feasible accuracy. The contact force generated at the contact point is based on a penalty contact force [8, 9]. Contact force can be calculated using the following relationship:

$$F_n = k_{con}\delta^{m_1} + c_{con}\frac{\dot{\delta}}{\left|\dot{\delta}\right|}\left|\dot{\delta}\right|^{m_2}\delta^{(m_3)} \tag{1.3}$$

where δ is the penetration, $\dot{\delta}$ is the penetration speed, k_{con} and c_{con} are the stiffness and the damping coefficients, respectively, m_1, m_2 and m_3 are the stiffness, the damping, and the indentation exponents, respectively. With this formulation, there are five parameters to be identified, namely $k_{con}, c_{con}, m_1, m_2, m_3$. In conclusion, nine parameters have to be defined, *i.e.* four regarding the rotational spring and five regarding the contact formulation, respectively. These parameters are divided into two groups: the first one contains the parameters linked to the stiffness characteristics ($k_\varphi, n_{k\varphi}$, k_{con}, m_1); the second one includes the parameters relating to the damping properties (c_φ, $n_{c\varphi}, c_{con}, m_2, m_3$). The first set influences the solution both in quasi-static conditions and dynamic, and the second set is relevant mainly in dynamic simulations.

Modifications for lightweight can be done essentially in two different ways: creating holes in the rim of the gear or reducing the gear thickness of the rim. Figure 1 reports the main geometrical parameters associated with a lightening solution. In particular, in the case of gear lightening by holes, the following geometric parameters can be identified: the number of holes *N*, the radius of the holes R_h and the radius of the circumference of the hole R_{ch} (Figure 1a). The rim thickness reduction, for generic spur gear, can be synthesized with four additional dimensions: t_2 is gear width, t_1 is section thickness, l_1 the crown height, l_2 the central height and l_3 the rim height (Figure 1b).

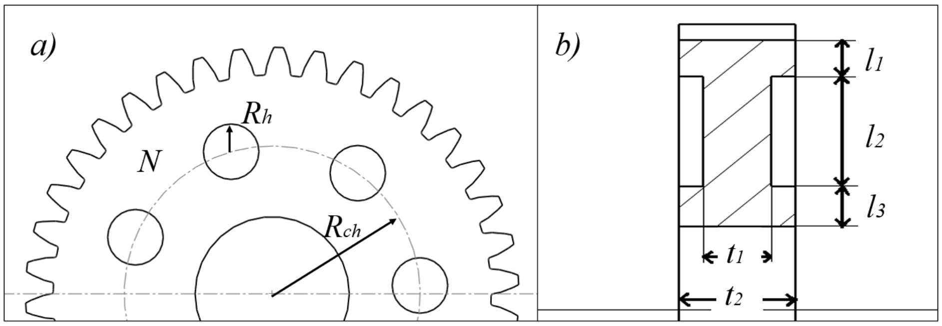

Figure 1 Lightening parameters

Numerical Example

A numerical example was carried out adopting two gears having identical macro geometry properties but different lightening conditions. In particular, the driving gear is considered without lightening conditions, while the driven gear is characterized both by reduction of the body thickness and by the presence of holes. Table 1 shows the geometric characteristics of both gears.

Table 1 Gear geometrical properties: A) general parameters B) lightning parameters

A)	Gear A	Nomenclature	UoM
m	1.5	*Module*	mm
Z	67	*Number of Teeth*	
d_p	100.5	*Pitch Circle Diameter*	mm
ϕ_p	20	*Pressure angle*	deg
a	1	*Addendum Coefficient*	mm
b	1.25	*Dedendum Coefficient*	mm
c	0.07	*Backlash*	mm
t_2	17	*Tooth Width*	mm
R_{fill}	0.45	*Fillet tooth radius*	mm

B)	Lightening modifications		
N	6	*Number of holes*	
R_h	6	*Hole radius*	mm
R_{ch}	32.36	*Position of holes*	mm
l_1	6.075	*External length*	mm
l_2	23.25	*Length of reduction*	mm
l_3	7.425	*Internal length*	mm
t_1	10	*Thickness reduction*	mm

In the example, the gears have been connected to the ground using revolute joints at the centres of the gears. A ramp motion is prescribed to the driving gear, while a similar ramp is adopted for the resistant torque applied to the driven gear to avoid impacts. Figure 2 shows the setup of the model. Contact stiffness parameters (k_{con} and m_1) are identified through a fit of the results from Weber's analytical solution [10]. Contact stiffness is not influenced by the lightening because it depends only on the geometrical profile and material of the gear. In this simulation $k_{con} = 5.64 \cdot 10^6$ N/mm; $m_1 = 1.24$.

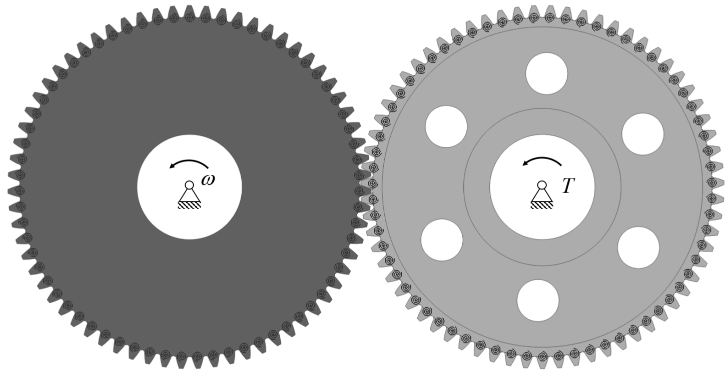

Figure 2 Numerical example setup

Spring coefficients of the unmodified gear are computed by adopting the methodology developed in [3]. In this simulation k_ϕ = $1.06{\cdot}10^6$ Nmm/rad; $n_1 = 1.1$. The spring coefficients of the lightened gear are computed with the same method, but the displacement of the tooth is obtained for each tooth through a set of FE models in which the gear has been considered fixed in the inner hole and loaded at the primitive circle. The results of the stiffness computation are reported in Figure 3. In particular, Figure 3a shows the adopted tooth enumeration, while Figure 3b reports the stiffness computed for each tooth. An interesting behaviour can be observed from this first FE result: the stiffness is higher in teeth positioned over the holed. It is apparently an unintuitive result but can be explained in the stress contour. The most stressed zone is not the portion under the tooth but the zone near the fillet radius.

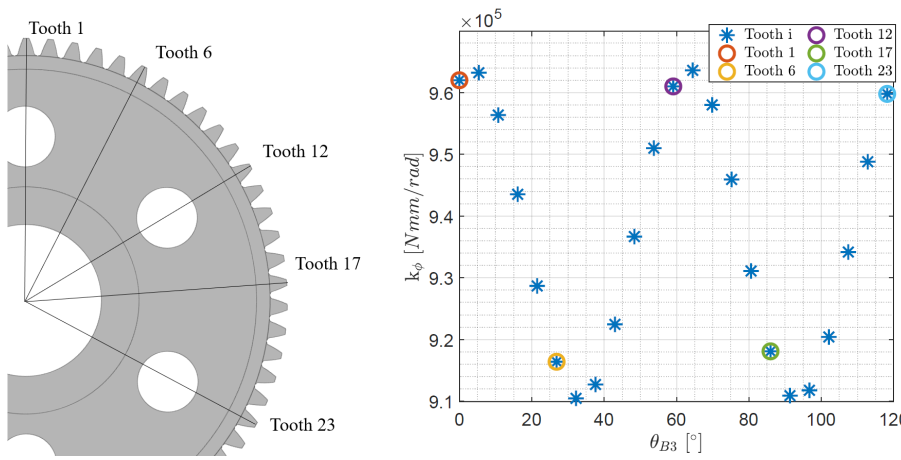

Figure 3 a) Tooth enumeration b) stiffness computed for each single tooth

Quasi-static results

For the quasi-static simulation, the ramp of motion starts from 0 rad/s at the time 0 s, and reaches 1.0 rad/s at time 0.001 s. The same ramp is adopted for the resisting torque applied to the driven gear: 0 Nm at 0 s, end 50 Nm at 0.001 s. The simulation end time is set to admit a 120 deg of gear rotation to highlight the effect of the holes on the STE. The same simulation conditions have been adopted in the reference model based on FE model, composed from 2D 4-side elements, under the assumption of planar strain. The contact formulation adopted for FE models, is a 2D contact between involute profiles based on the concept of hard contact. As the result, a comparison among FE models and MUBOCOF models is reported in Figure 4. In particular, Figure 4a reports the STE computed from 0 to 120 deg to highlight the effects of the holes, while Figure 4b highlights a magnification of the STE from 20 to 40 deg to better underline the comparison. The effects of the holes can be replicated in a satisfactory approximation. The only difference between FE and MUBOCOF is the amplitude of the STE. It can be attributed to an overestimation of the stiffness

Materials Research Proceedings **26** (2023) 659-664 https://doi.org/10.21741/9781644902431-106

when two couple of the teeth are in contact. In fact, MUBOCOF does not consider the coupling effect in deformation due to the foundation.

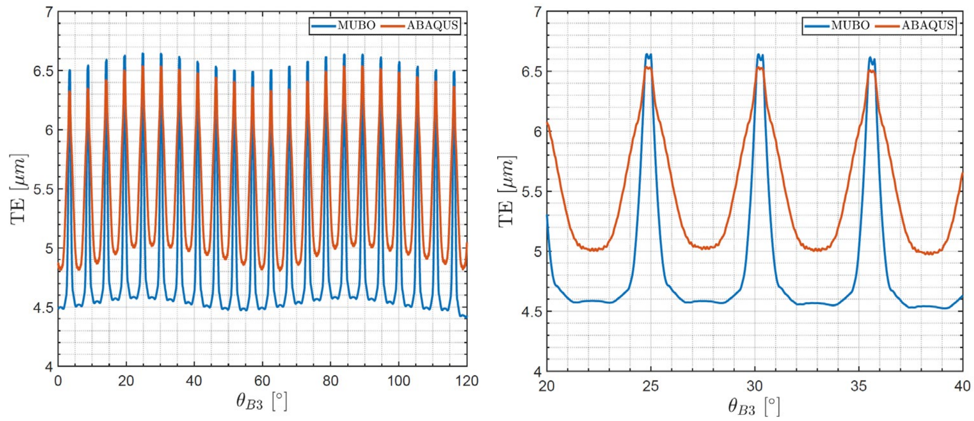

Figure 4 a) STE computed for 120 deg; b) STE magnification

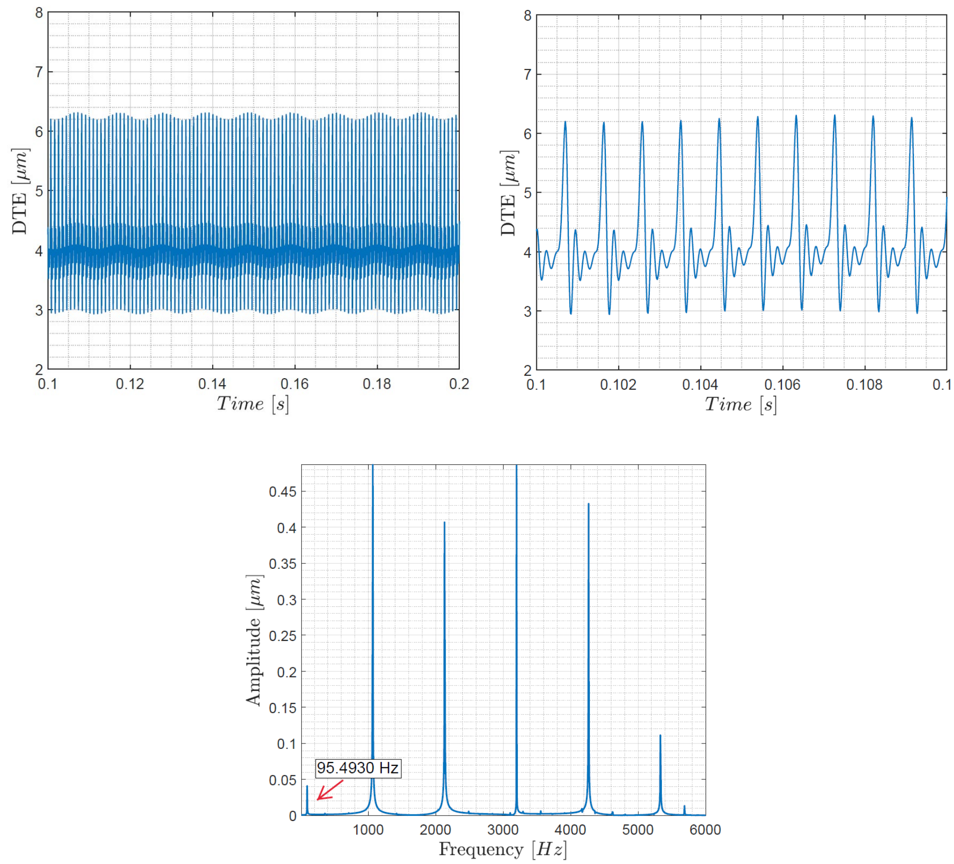

Figure 5 a) DTE signal; b) Magnification of DTE; c) Fast Fourier Transform of DTE

Dynamic analysis

In the dynamic simulation, all the parameters have been maintained except the ramp for the motion and the applied torque. The ramp of motion begins from 0 rad/s at the time 0 s, and reaches 100 rad/s at time 0.01 s. The ramp for the resisting torque applied to the driven gear is 0 Nm at 0 s, end 50 Nm at 0.01 s. Figure 5 summarizes the DTE results. The total simulation time is set to 0.2 s. Figure 5a reports the DTE signal in which the transient phase is avoided. It can be observed the vibration component generated from the holes is maintained. Moreover, the additional vibration component due to the oscillation of the teeth is introduced (Figure 5a). A very interesting plot is reported in Figure 5c in which the Fast Fourier Transform (FFT) of the DTE signal is reported. It can be seen how the first peak represents the vibration component induced by the holes.

Conclusions

In this paper, a preliminary study of the LGs through a MUBOCO-PR is performed. TE results in quasi-static conditions demonstrate a good agreement with the FE method. STE results highlight a slight difference in STE value when multiple teeth are in contact. The effects due to the variation of the stiffness with respect to the angular position are correctly identified. Dynamic analysis shows how the vibration induced from the flexibility of the tooth generates an additional oscillating component and a dynamic amplification of the TE.

This research is funded by MUR through the PRIN *"Innovative contact-based multibody model for noise and vibration prediction in high-performance gears"*. Code project: 202022Y4N5.

References

[1] S. Shweiki, A. Palermo and D. Mundo, "A Study on the Dynamic Behaviour of Lightweight Gears," *Hindawi Shock and Vibration,* vol. 2017, p. 12, 2017. https://doi.org/10.1155/2017/7982170

[2] S. Shweiki, A. Rezayat, T. Tamarozzi and D. Mundo, "Transmission Error and strain analysis of lightweight gears by using a hybrid FE-analytical gear contact model," *Mechanical Systems and Signal Processing,* pp. Volume 123, Pages 573-590, 2019. https://doi.org/10.1016/j.ymssp.2019.01.024

[3] M. Cirelli, P. P. Valentini and E. Pennestrì, "A study of the non-linear dynamic response of spur gear using a multibody contact based model with flexible teeth," *Journal of Sound and Vibration,* 2019. https://doi.org/10.1016/j.jsv.2019.01.019

[4] M. Cirelli, P. P. Valentini and E. Pennestrì, "Multibody dynamics of gear pairs: comparison among different models," in *Proceedings of the 8th ECCOMAS Thematic Conference on MULTIBODY DYNAMICS*, Prague, 2017.

[5] M. Cirelli, O. Giannini, P. P. Valentini and E. Pennestrì, "Influence of tip relief in spur gears dynamic using multibody models with movable teeth," *Mechanism and Machine Theory,* vol. 152, no. 103948, 2020. https://doi.org/10.1016/j.mechmachtheory.2020.103948

[6] S. Harris, "Dynamic loads on the teeth of spur gears," *Proceedings of the Institution of Mechanical Engineering,* vol. 172, p. 87, 1958. https://doi.org/10.1243/PIME_PROC_1958_172_017_02

[7] J. Choi, H. S. Ryu, C. W. Kim and J. H. Choi, "An efficient and robust contact algorithm for a compliant contact force model between bodies of complex geometry," *Multibody Syst Dyn,* vol. 23, p. 99–120, 2010. https://doi.org/10.1007/s11044-009-9173-3

[8] J. Choi, S. Rhim and J. H. Choi, "A general purpose contact algorithm using a compliance contact force model for rigid and flexible bodies of complex geometry," *International Journal of Non-Linear Mechanics,* vol. 53, pp. 12-23, 2013. https://doi.org/10.1016/j.ijnonlinmec.2013.01.017

[9] M. Machado, P. Moreira, P. Flores and H. M. Lankarani, "Compliant contact force models in multibody dynamics Evolution of the Hertz contact theory," *Mechanism and Machine Theory,* vol. 53, p. 99–121, 2012. https://doi.org/10.1016/j.mechmachtheory.2012.02.010

[10] C. Weber, "The Deformations of Loaded Gears and The Effect on Their Load-Carrying Capacity," *British Dept. of Scientific and Industrial Research,* vol. Report No.3, 1949.